Numerical Research of Compressible Turbulent Swirl Flow with Energy Separation in a Cylindrical Tube

Jela M. Burazer

Research Assistant
University of Belgrade
Faculty of Mechanical Engineering

Đorđe M. Novković

PhD Student
University of Belgrade
Faculty of Mechanical Engineering

Darko M. Knežević

Associate Professor
University of Banja Luka
Faculty of Mechanical Engineering
Bosnia and Herzegovina

Milan R. Lečić

Professor
University of Belgrade
Faculty of Mechanical Engineering

The aim of this paper is to numerically analyze the energy separation phenomenon in turbulent compressible swirling flow in a cylindrical tube. In that sense, the energy separation in a vortex tube with orifice at cold end closed completely is examined numerically using OpenFOAM software. Obtained results are validated with the experimental ones. For numerical calculations, both two-equation (standard k-ε) and full Reynolds stress turbulence models (LRR) are used. The computational domain is considered to be two-dimensional, and the working fluid – air is treated as calorically perfect gas. Mesh independence test is carried out for four different mesh sizes. Distributions of swirling flow intensity, average swirl and angular velocity clearly show the influence of the swirl presence in the flow. The values of these quantities point to the physics of this extremely complex flow-thermodynamic phenomenon, such is the energy separation. Based on values and distributions of these flow quantities a comparison between incompressible and compressible turbulent swirling flow is performed.

Keywords: vortex tube, energy separation, swirl, turbulence, OpenFOAM.

1. INTRODUCTION

Energy separation is a spontaneous process of total energy redistribution in the fluid flow. A device that has become famous because of this phenomenon is called vortex tube. It is a simple device with no moving parts that separates compressed gas stream into cold and hot streams exiting on the opposite sides of the vortex tube. The compressed gas enters the tube in the way that the swirling flow is formed in this device. Since there are no moving parts, the energy separation effect can only be attributed to the fluid dynamics effects. Nevertheless, the explanation of this phenomenon is still ambiguous.

Ranque-Hilsch vortex tube is discovered by accident by Ranque [1] in 1933, and improved by Hilsch [2] in 1946. Since these pioneering papers, extensive work has been performed in order to describe the fluid flow and thermodynamics present in this device. Since this is a device of small dimensions, experimental measurements inside the fluid flow domain is very difficult. A great step forward is made by introducing the CFD analysis in the research. Fröhlingsdorf and Unger [3] published one of the first papers regarding the CFD analysis of the vortex tube performance. In Behera et al. [4], Eiamsa-ard [5], Shamsoddini et al. [6], Avci et al. [7], Hamdan et al. [8], Khazei et al. [9], Manimaran [10, 11] efforts are made to describe the possibilities of vortex tube efficiency improvement by changing its geometric parameters. Ouadha et al. [12], Han et al. [13], Agrawal et al. [14],

Thakare et al. [15, 16] described the influence of the thermophysical properties of the gases that are used in vortex tubes on their performance. According to these research the L/D ratio should be as high as possible, but not over $L/D = 45$. Further increase of the L/D value has no effect on the performance of vortex tube. Increase of the number of nozzles has positive effect on energy separation in vortex tube. Their location should be as close as possible to the orifice. Higher inlet to cold outlet pressure ratio yields greater energy separation, but there is also an optimum value. All reported CFD research is performed by using commercial software. Burazer et al. [17] used open-source software in their vortex tube research. A new solver within OpenFOAM was developed, that enabled numerical prediction of energy separation in different fluid flows [18].

This paper deals with the energy separation in a swirling compressible flow in a tube that is a theoretical model of a vortex tube. Namely, the orifice of the vortex tube considered in this paper is closed completely. Nume–rical computations are performed within OpenFO-AM, an open-source CFD software. The same solver developed in [17] is used here, together with standard k-ε and LRR turbulence models. The main goal is to determine the possibilities for energy separation in such flow conditions. Integral flow parameters such are swirl and angular velo–city are presented in this research. Also, a downstream distribution of the swirl flow intensity in this compressible turbulent swirling pipe flow is analyzed.

2. MATHEMATICAL MODELING

Vortex tube flow is turbulent and highly compressible, with high swirl. Having that in mind, the equations that govern the fluid flow are the Favre averaged continuity equation:

$$\partial_t \langle \rho \rangle + \nabla \cdot \left(\rho \underline{\tilde{u}} \right) = 0 \qquad (1)$$

Favre averaged Navier-Stokes (FANS) equations:

$$\begin{aligned} &\partial_t \left(\langle \rho \rangle \underline{\tilde{u}} \right) + \nabla \cdot \left(\langle \rho \rangle \underline{\tilde{u}} \otimes \underline{\tilde{u}} \right) \\ &= -\nabla \langle p \rangle + \nabla \cdot \left(\langle \underline{\underline{T}} \rangle - \langle \rho \underline{u}'' \otimes \underline{u}'' \rangle \right) \end{aligned} \qquad (2)$$

and Favre averaged total energy equation:

$$\begin{aligned} &\partial_t \left(\langle \rho \rangle \tilde{H} \right) + \nabla \cdot \left(\langle \rho \rangle \tilde{H} \underline{\tilde{u}} \right) \\ &= \partial_t \langle p \rangle + \nabla \cdot \left[-\langle \rho \underline{u}'' h'' \rangle + \langle \underline{\underline{T}} \cdot \underline{u}'' \rangle - \left\langle \rho \underline{u}'' \frac{1}{2} \underline{u}'' \cdot \underline{u}'' \right\rangle \right] \\ &+ \nabla \cdot \left[\underline{\tilde{u}} \cdot \left(\langle \underline{\underline{T}} \rangle - \langle \rho \underline{u}'' \otimes \underline{u}'' \rangle \right) \right] - \nabla \cdot \underline{\tilde{q}}. \end{aligned} \qquad (3)$$

This set of equations is not closed. For doing that, we need constitutive equations that are also Favre ave–raged [17]. The concept of Favre averaging is intro–duced in the modeling of turbulent compressible flow. It is purely mathematical, since the aim is to avoid the density fluctuations in equations. Nevertheless, density fluctuations influence on the fluid flow is not excluded from the equations.

Apart from the Reynolds stress tensor $-\langle \rho \underline{u}'' \otimes \underline{u}'' \rangle$, there are few more unknown terms in the listed equa–tions. These are turbulent heat flux vector $-\langle \rho \underline{u}'' h'' \rangle$, molecular diffusion $\langle \underline{\underline{T}} \cdot \underline{u}'' \rangle$ and turbulent transport $-\langle \rho \underline{u}'' 0.5 \underline{u}'' \cdot \underline{u}'' \rangle$. Like Reynolds stresses, these unknowns are modeled. More about the modeling of these terms can be found in Ref. [17]. The most common approach for turbulence modeling is the Bou-ssinesq approximation, which is the basis of the two-equation models. One of the representatives of these models, namely standard k-ε model, is used for compu–tations in this work. Another model, which solves additional equations for each of the Reynolds stress components is the Launder-Reece-Rodi stress model (LRR). Details about these two models can be found in [21, 22].

This paper presents the results obtained by nume–rical computations in an open-source software named OpenFOAM. This software is a big set of C++ libraries intended for numerical computations in continuum mechanics. It has a text user interface, and every part of the code is available to the user. Community-driven version foam-extend-3.1 is used for all computations in this paper. Transient density-based solver named rhoCentralTurbFoam is used for computations. This is a compressible solver that is based on the central differencing scheme of Kurganov and Tadmor [23]. More details about this solver can be found in [17]. This problem is also considered as steady-state in [24], but results from transient calculations proved to be better. Hence, this paper presents only transient solver results.

3. DESCRIPTION OF THE EXPERIMENT AND NUMERICAL CASE SET-UP

The vortex tube that is used for the present research is the one from Hartnett and Eckert [19]. This is a vortex tube with diameter $D = 2R = 0.0762$ m, and length $L = 0.77$ m. The orifice is completely closed and

swirling flow is generated by injecting gas through eight nozzles equally spaced around the circumference of the tube. Nozzle diameter is 9.525 mm. The same is the width of the exit on the opposite side of the tube downstream. Computational domain used in compu–tations is displayed in Figure 1. Since there are eight nozzles for swirl generation, it is justified to assume that the flow inside the tube is axisymmetric. In order to reduce the computation effort needed for calculations, numerical computations are performed on the so-called wedge geometry. More about wedge geometry can be found in [25].
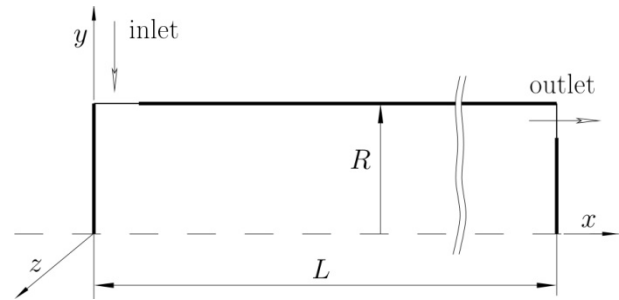

Figure 1. Computational domain.

A block structured mesh generator blockMesh avai–lable within OpenFOAM is used for mesh generation. Mesh is graded in parts of the flow where high gradients of physical quantities are expected. Part of the com–putation mesh is presented in Figure 2. Dimensionless distance from the wall is carefully considered. Since standard k-ε model is used in computations, $y+$ should be of the order of 30. This is confirmed after the calculations are completed.
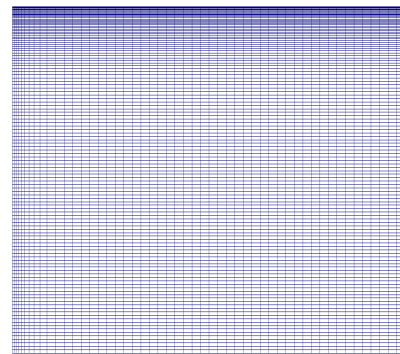

Figure 2. Part of the computational mesh at the inlet.

Boundary conditions are set as follows. At the inlet, a fixed value of temperature and velocity are set, while for pressure zeroGradient boundary condition is set. It is assumed that the turbulence intensity is of the order of 5% of the averaged velocity and that the integral scale of turbulence is 10% of the inlet dimension. Based on that, values of the turbulence quantities are calculated. On the outlet, only for pressure is set fixed value. For velocity, temperature and turbulence quantities, a zeroGradient boundary condition is set. A zero value of the velocity vector is set on the walls of the tube. On this boundary surface, for all other physical quantities, zeroGradient boundary condition is set. On the sides of the wedge geometry, a wedge boundary condition is set.

The size of a time step is controlled by setting the maximal value of Courant number, $Co_{max} = 0.3$. Discre–

tization of all equation terms is performed by using the second order schemes. Tolerances for residuals of all physical quantities except velocity is set to 10^{-10}, while for velocity this tolerance is set to 10^{-9}. Relative tole–rance is set to zero for all quantities.

The air that is injected in vortex tube is considered to be calorically perfect gas width Prandtl number $Pr = 0.7$, and specific heat $c_p = 1004.5$ J/(kgK).

4. RESULTS AND DISCUSSION

4.1 Mesh independence study analysis

The analysis of the mesh size influence on the conver–gence of the computations is performed. The calcu–lations are conducted on four different mesh sizes with 24000 (M0), 37050 (M1), 52500 (M2) and 78400 (M3) cells. It is adopted that the total temperature distribution in a single cross section is the key parameter for the mesh independence study. The influence of the mesh size on numerical results is shown in Figure 3. Com–putations performed on the M0 mesh did not have a converged solution.
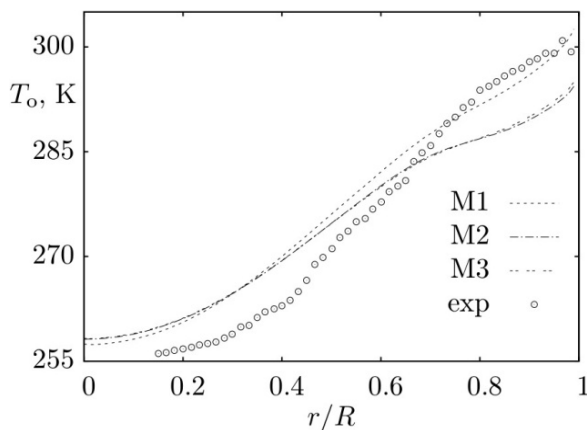

Figure 3. Mesh independence study results, cross section *x/D* = 0.333.

It is obvious from Figure 3 that the results from meshes M2 and M3 practically coincide. The results of computations performed on mesh M1 are different, especially in the wall area of the tube. Based on pre–vious considerations, it is concluded that all compu–tations in this research are to be performed on mesh M2. These results are presented in this paper.

4.2 Validation of turbulence models' results

The same vortex tube considered in this paper was the subject of the research presented in Ref. [20]. In that research, numerical computations were performed using standard k-ε and algebraic stress models. It was con–cluded that the stress model gives better results. This is confirmed in this paper.

Fields that are important in the consideration of a vortex tube flow are velocity and total temperature fields. Firstly, we will examine the ability of turbulence models to predict velocity field in this compressible turbulent flow with extremely pronounced swirl. In the first cross section considered, i.e. the one that is the closest to the tube's inlet, $x/D = 0.333$, both turbulence models predict Rankine vortex (see Figure 4). Indeed,

experimental results from Ref. [19] also show Rankine vortex flow in this cross section of the flow domain.

Circumferential velocity distribution in cross sections $x/D = 2$ and $x/D = 6$ reveals the presence of a forced vortex flow. The discrepancy between the expe–rimental and computational values is smaller in cross section that is closer to the inlet of the tube. Compared to the experimentally obtained values [19], compu–tational results predict higher values of the circum–ferential velocity in the shear layer of the flow field.
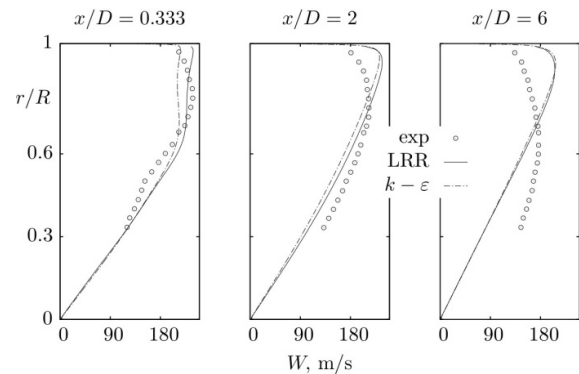

Figure 4. Circumferential velocity *W* distribution in three cross sections of the tube.

Radial distribution of total temperature in three cross sections of the tube is presented in Figure 5. The best agreement between the experimental and computatio–nally obtained results is accomplished in cross section $x/D = 2$, while the greatest discrepancy between these results is obtained in the cross section closest to the tube's exit ($x/D = 6$).
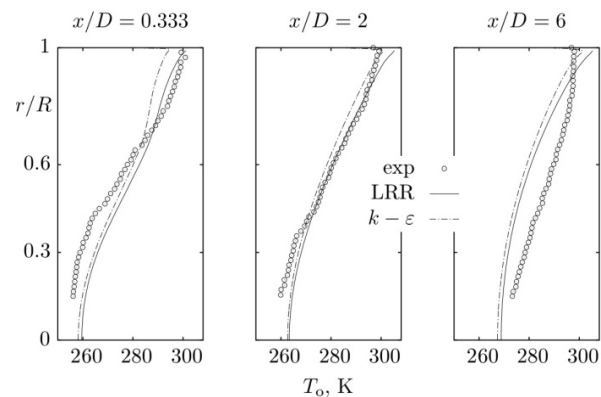

Figure 5. Radial distribution of total temperature in three cross sections of the vortex tube.

Both turbulence models, as well as the experiments, confirmed the presence of the energy separation pheno–menon in the tube. The minimum of total temperature is in the coaxial part of the tube, while the maximum value - higher than the inlet value of the total temperature is in the shear part of the swirling flow (see Figure 6).
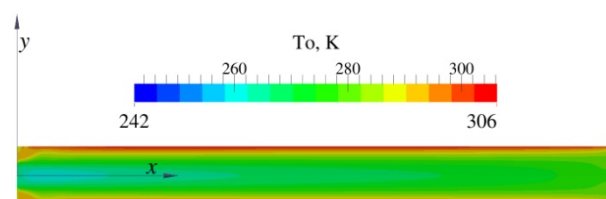

Figure 6. Total temperature distribution in vortex tube, LRR full Reynolds stress turbulence model.

Since the total temperature separation in this flow is of greater importance than the velocity distribution, the main factor in selection of the better computational model is better prediction of the temperature field. Hence, the full Reynolds stress turbulence model - LRR is appointed as the better one, and with this model's results further analysis will be performed in this paper.

4.3 Analysis of the integral flow parameters distributions using full RSTM

Since we are dealing with swirling flow of air, one of the first things that has to be assessed is the swirl strength in this flow. There are many ways to describe this quantity. Namely through swirl flow parameter S, swirl number Ω, swirl flow intensity θ etc. [26]. The last is appropriate for use in this research, since we are dealing with swirling flow in a tube. Swirl flow intensity is calculated following:

$$\theta = \frac{\int_0^R \rho r U W^2 \mathrm{d}r}{\int_0^R \rho r U^3 \mathrm{d}r}. \quad (3)$$

Basically, this is the ratio between the fluxes of kinetic energies in the circumferential and axial direction of the flow. Figure 7 depicts downstream distribution of swirl flow intensity in the tube with swirling turbulent compressible air flow. Since the orifice of this vortex tube is closed, it is evident that the kinetic energy in the axial direction is higher than in the case of a classic vortex tube [24]. More importantly, even though we are dealing with compressible flow, the swirl decay law is the same as in the case of the incompressible swirling flow in a tube [27].
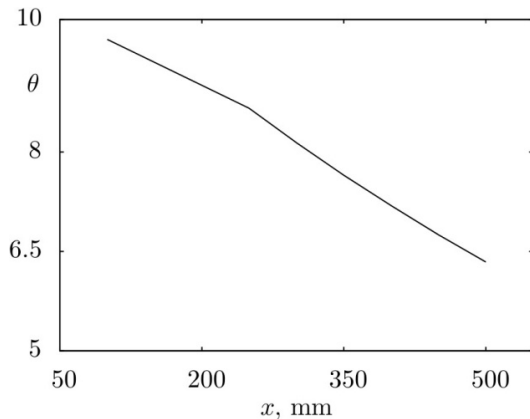

Figure 7. Downstream distribution of swirl flow intensity θ.

From the axial velocity distribution presented in Figure 8, it is obvious that in the cross section $x/D = 0.333$ ($x = 25.4$ mm) there is a reverse flow in the coaxial part of the flow domain. Also, there is severe increase in the axial velocity intensity in this cross section in respect to the other cross sections considered. This is the consequence of the closed orifice - the place where the cooled air leaves the tube. Since the orifice is closed, the cooled air has nowhere to escape from the tube. Hence, there is no reverse flow downstream, and the axial velocity has higher values comparing to the case when the central opening in the vortex tube is not

closed. The value of the axial velocity is rising downstream the tube.

Extremely high values of the swirl flow intensity in present study in comparison to the incompressible swirling flow in tube [27] point to full domination of the centrifugal force on the turbulent transport and energy transfer mechanism. There is a breaking point in the downstream distribution of the swirling flow intensity θ approximately at $x = 250$ mm ($x/D = 3.3$)
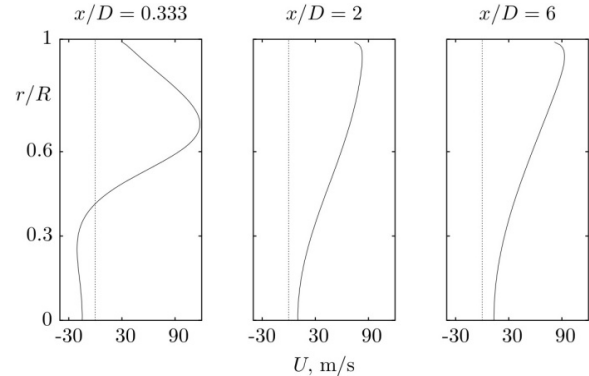

Figure 8. Radial distribution of the axial velocity U in cross sections $x/D = 0.333$, $x/D = 2$ and $x/D = 6$.

Circulation of the circumferential velocity Γ is important parameter from the point of view of vorticity content in the flow. This quantity points to existence or absence of vortices i.e. singularities like vortex lines in the flow fields. Circulation displays the intensity of that vortices. Circulation is defined as

$$\Gamma = \int_0^{2\pi} W r \mathrm{d}\varphi, \quad (4)$$

from which it follows $\Gamma = 2\pi\omega r^2$ for $r \le R_w$ while for $r \ge R_w$ it stands $\Gamma = 2\pi\omega R_w$. Here R_w is the radius of the border streamline that is between the forced and potential swirl. In this paper this is simplified and instead of circulation Γ, distribution of swirl rW is presented. The main reason for this simplification is the comparison of the swirl rW distribution in vortex tube compressible swirl flow and incompressible swirl flow that is present in the tube in which the swirl is generated by axial fan.
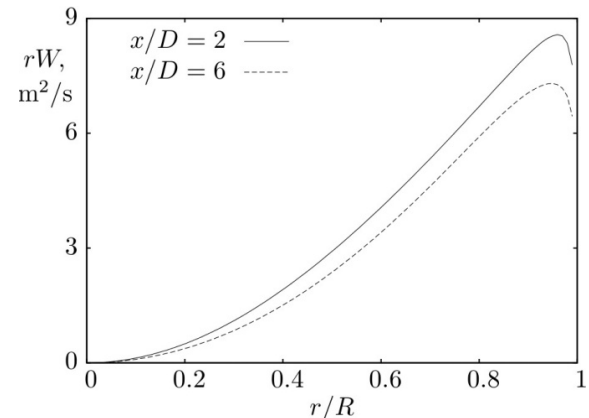

Figure 9. Swirl distribution in the radial direction in two cross sections of the vortex tube.

Distribution of swirl rW in this specific case of a vortex tube with orifice closed is displayed in Figure 9.

It is evident that this quantity shows slow decay downstream the vortex tube. Maximum value of swirl rW is in the shear layer of the swirling flow. In comparison to the case of an incompressible swirling flow present in the tube behind axial fan presented in Ref. [28], it is obvious that there are some differences in swirl distributions. In incompressible swirling flow behind axial fan that rotates at 1500 min^{-1}, the value of the maximum swirl is about ten times smaller than in the case of the vortex tube compressible swirling flow presented in this research. This is evident even by comparing the magnitude of the angular velocities in these two cases of the flow field. On the other hand, in the vortex tube flow there is no region of constant swirl ($rW \approx$ const), unlike in the case of the incompressible fan swirl flow case [28].

Radial distribution of the angular velocity in two cross sections of this vortex tube is presented in Figure 10. The influence of the viscosity is obvious in the wall region. Hence, there is a drop in the value of angular velocity in both cross sections. Radial decrease of the angular velocity in the cross section $x/D = 2$ is decreasing towards the tube's wall. However, in the cross section $x/D = 6$ there is a slight increase in the angular velocity value from the vortex core towards the shear layer region. Afterwards, there is a region of approximately constant value of this quantity. In the wall region the viscosity forces the angular velocity to drop to zero value.
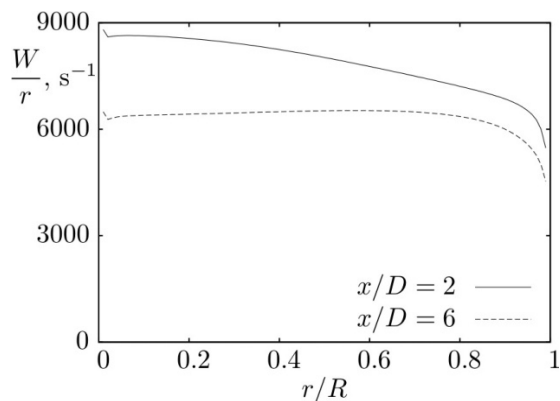
Figure 10. Radial distribution of the angular velocity in the two cross sections of the vortex tube.

When maximum values of angular velocity in this research and the one from Ref. [28] are compared, it is obvious that the values reported here are approximately 30 times greater. These extremely higher values of the swirl and angular velocity presented in this study, in comparison to the incompressible swirling flow in tube [28], once again point to full domination of the centri–fugal force on the turbulent transport and energy trans–fer mechanism. Consequently we can search for the rea–son of the energy separation presence in the fluid flow.

5. SUMMARY

Numerical analysis of energy separation phenomenon in turbulent compressible swirling flow in a cylindrical tube is performed in this research. The aim of the paper is to show that even in this flow geometry there is a possibility for energy separation occurrence. OpenFO-

AM solver is capable of capturing this phenomena here also. Reynolds stress models predict better total tempe–rature field, what is a confirmation of previously re–ported research of other authors.

It is proved that the swirl decay law in this, compressible turbulent swirling flow corresponds to the case of the incompressible turbulent swirling flow in a cylindrical tube. There is, however, significant diffe–rence in the intensity of the swirl in these two flow cases. Distributions of swirl rW and angular velocity W/r in this specific case of a vortex tube, with orifice closed, are displayed and compared with the case of an incompressible swirl flow in a tube, where the swirl is generated by axial fan. Higher values of these quantities are reported in compressible swirl flow. It is noted that in vortex tube flow there is no region of constant swirl i.e. $rW \approx$ const.

These results will, hopefully, help in constituting more reliable conclusions about the physics of the ene–rgy separation phenomenon present in vortex tubes as well as in other flow fields.

REFERENCES

[1] Ranque, G: Experiments on Expansion in a Vortex With Simultaneous Production of a Hot Air Exhaust and a Cold Air Exhaust, J. Phys. Radium, Vol. 4, No. 7, pp. 112 - 114, 1933, (in French)

[2] Hilsch, R: The Use of the Expansion of Gases in a Centrifugal Field as Cooling Process, Rev. Sci. Instrum, Vol. 18, No. 2, pp. 108-113, 1947.

[3] Fröhlingsdorf, W, Unger, H: Numerical Investi–gations of the Compressible Flow and the Energy Separation in the Ranque-Hilsch Vortex Tube, Int. J. of Heat and Mass Transfer, Vol. 42, No 3, pp. 415 - 422, 1999.

[4] Behera, U, Paul P. J, Kasthurirengan S, Karunanithi R, Ram S, Dinesh K, Jacob S: CFD Analysis and Experimental Investigation Towards Optimizing the Parameters of Ranque-Hilsch Vortex Tube, Int. J. of Heat and Mass Transfer, Vol. 48, No. 10, pp. 1961-1973, 2005.

[5] Eiamsa-ard S: Experimental investigation of energy separation in a counter-flow Ranque-Hilsch vortex tube with multiple inlet snail entries. International Communications in Heat and Mass Transfer, Vol. 37, No. 6, pp. 637 - 643, 2010.

[6] Shamsoddini, R., Nezhad, A. H: Numerical Anal–ysis of the Effect of Nozzles Number on the Flow and Power of Cooling of a Vortex Tube, Int. J. of Refrigeration, Vol. 33, No. 4, pp. 774-782, 2010.

[7] Avci M: The effects of nozzle aspect ratio and nozzle number on the performance of the Ranque-Hilsch vortex tube, Applied thermal engineering, Vol. 50, No. 1, pp. 302 - 308, 2013.

[8] Hamdan M. O, Alsayyed B, Elnajjar E: Nozzle parameters affecting vortex tube energy separation performance. Heat mass transfer, Vol. 49, No. 4, pp. 533 - 541, 2013.

[9] Khazei, H, Teymourtash A. R, Malek-jafarian M, Effects of Gas Properties and Geometrical Parameters on Performance of a Vortex Tube, Scientia Iranica, Transactions B: Mechanical Engineering, Vol. 19, No. 3, pp. 454-462, 2012.

[10] Manimaran R: Computational analysis of energy separation in a counter-flow vortex tube based on inlet shape and aspect ratio. Energy, Vol. 107, pp. 17 - 28, 2016.

[11] Manimaran R: Computational analysis of flow features and energy separation in a counter-flow vortex tube based on number of inlets. Energy, Vol. 123, pp. 564 - 578, 2017.

[12] Ouadha A, Baghdad M, Addad Y: Effect of variable thermophysical properties on flow and energy separation in a vortex tube. International Journal of refrigeration, Vol. 36, No. 8, pp. 2426 - 2437, 2013.

[13] Han X, Li N, Wu K, Wang Z, Tang L, Chen G, Xu X: The influence of working gas characteristics on energy separation of vortex tube, Applied thermal engineering, Vol. 61, No. 2, pp. 171 - 177, 2013.

[14] Agrawal N, Naik S. S, Gawale Y. P: Experimental investigation of vortex tube using natural substances. International Communications in Heat and Mass transfer, Vol. 52, pp. 51 - 55, 2014.

[15] Thakare H. R, Parekh A. D: CFD analysis of energy separation of vortex tube employing different gases, turbulence models and discretisation schemes. International Journal of heat and mass transfer, Vol. 78, pp. 360 - 370, 2014.

[16] Thakare H. R, Parekh A. D: Computational analysis of energy separation in counter-flow vortex tube, Energy, Vol. 85, No. 62 - 77, 2015.

[17] Burazer J. M, Ćoćić A. S, Lečić M. R: Numerical research of the compressible flow in a vortex tube using OpenFOAM software, Thermal Science, Vol. 21, Suppl. 3, pp. S745-S758, 2017.

[18] Burazer J. M: Numerical research of energy separation in a cylinder wake, in *Proceedings of the 6th International Congress of Serbian Society of Mechanics, Turbulence Minisymposium*, Mountain Tara, Serbia, June 19 - 21. 2017, Paper M2i.

[19] Hartnett J. P, Eckert E. R. G: Experimental study of the velocity and temperature distribution in a high-velocity vortex-type flow, Trans. ASME, Ser. C, J. Heat Transfer Vol. 79, pp. 751-758, 1957.

[20] Eiamsaard S., Promvonge P: Numerical inv-sti–gation of the thermal separation in a Ranque-Hilsch vortex tube, International Journal of Heat and Mass Transfer Vol. 50, No. (5-6), pp. 821-832, 2007.

[21] Launder, B., Sharma, B: Application of the Energy Dissipation Model of Turbulence to the Calculation of Flows Near a Spinning Disk, Letters in Heat and Mass Transfer, Vol. 1, No. 2, pp. 131-138, 1974.

[22] Launder B. E, Reece G. J, Rodi W: Progress in the development of a Reynolds-stress turbulence closure, J. Fluid Mech. Vol. 68, No. 3, pp. 537-566, 1975.

[23] Kurganov A, Tadmor E: New high-resolution central schemes for nonlinear conservation laws and convection-diffusion equations, Journal of Computational Physics, Vol. 160, No. 1, pp. 241-282, 2001.

[24] Burazer J. M: *Turbulent compressible flow in a Ranque-Hilsch vortex tube*, Doctoral Dissertation, Faculty of Mechanical Engineering, University of Belgrade, 2017, (in Serbian)

[25] Greenshields C. J. OpenFOAM, The Open Source CFD Toolbox User Guide. Version 3.0.1, 2015.

[26] Benišek, M. H, Ilić D. B, Čantrak Dj. S, Božić I. O, Investigation of the turbulent swirl flows in a conical diffuser, Thermal Science, Vol. 14. Suppl, pp. S141-S154, 2010.

[27] Vukašinović B: *Turbulent transport and problems of its modeling in swirling flow*, Master thesis, Faculty of Mechanical Engineering, University of Belgrade, 1996, (in Serbian)

[28] Čantrak Đ. S: *Analysis of the vortex core and turbulence structure behind axial fans in a straight pipe using PIV, LDA and HWA methods*, Doctoral Dissertation, Faculty of Mechanical Engineering, University of Belgrade, 2012, (in Serbian)

NOMENCLATURE

D	diameter of the tube
H	total enthalpy
h	static enthalpy
k	kinetic energy of turbulence, $k = 0.5 u_i u_i$
L	length of the tube
p	pressure
$\underline{u}$	mean velocity vector
$\underline{\underline{T}}$	viscous stress tensor
T_o	total temperature
t	time
(x, y, z)	Cartesian coordinates
(x, r, φ)	cylindrical coordinates
U, V, W	mean velocities in axial (x), radial (r) and circumferential (φ) directions
$\underline{q}$	heat flux vector, $\underline{q} = -\lambda \nabla T$
$\langle \ldots \rangle$	time-average of …
$\widetilde{(\ldots)}$	Favre averaged of …
$(\ )''$	fluctuations due to density change
$\underline{(\ )}$	vector
$\underline{\underline{(\ )}}$	second-order tensor

$\partial_i f = \partial f / \partial x_i$

Greek symbols

ε	dissipation of kinetic energy of turbulence
θ	swirl flow intensity

ρ	fluid density
∇	gradient operator

Abbreviations

RSTM	Reynolds stress turbulence model
LRR	Launder-Reece-Rodi

НУМЕРИЧКО ИСТРАЖИВАЊЕ СТИШЉИВОГ ТУРБУЛЕНТНОГ ВИХОРНОГ СТРУЈАЊА СА РАСЛОЈАВАЊЕМ ПОЉА ТОТАЛНЕ ТЕМПЕРАТУРЕ У ЦЕВИ

Ј.М. Буразер, Ђ.М. Новковић, Д.М. Кнежевић, М. Р. Лечић

Циљ овог рада је нумеричка анализа феномена раслојавања поља тоталне температуре у турбулен-тном стишљивом вихорном струјању у цилин-дричној цеви. У том смислу, раслојавање поља тота-лне температуре у вртложној цеви са потпуно затвореним отвором за излаз охлађеног гаса се анализира нумеричким путем применом софтвером отвореног типа - OpenFOAM. Валидација добијених нумеричких резултата је вршена поређењем са вредностима добијеним експерименталним путем. За нумеричке прорачуне користе се двоједначински модел (стандардни *κ-ε*) и пуни напонски модел турбуленције (LRR). Прорачунски домен се сматра дводимензионалним, а радни флуид - ваздух третира се као калорички идеални гас. Утицај броја ћелија у мрежи је извршен помоћу четири различите вели–чине мреже. Расподеле јачине вихора, средњег ви–хора и угаоне брзине јасно указују на утицај присуства вихора у струјном пољу. Са друге стране, здружено са њиховом вредношћу упућују и на физику овог изузетно комплексног струјно-термо-динамичког феномена какав је феномен раслојавања поља тоталне температуре. На основу вредности и расподела ових струјних величина, извршено је и поређење између стишљивог и нестишљивог тур–булентног вихорног струјања.